Available online at www.sciencedirect.com
SCIENCE DIRECT®
Journal of Sound and Vibration 278 (2004) 637–655
JOURNAL OF SOUND AND VIBRATION
www.elsevier.com/locate/jsvi

Natural frequencies and mode shapes of flexural vibration of plates: laser-interferometry detection and solutions by Ritz's method

F.J. Nieves[a], F. Gascón[a], A. Bayón[b,*]

[a] *Departamento de Física Aplicada II, Universidad de Sevilla, E. T. S. de Arquitectura, Reina Mercedes 2, ES-41012 Sevilla, Spain*

[b] *Departamento de Física Aplicada a los Recursos Naturales, Universidad Politécnica de Madrid, E. T. S. I. Minas, Ríos Rosas 21, ES- 28003 Madrid, Spain*

Received 13 March 2003; accepted 13 October 2003

Abstract

This paper presents an experimental and theoretical study of flexural symmetric vibration modes of a linear elastic plate. A laser interferometer is used as detector of the free vibration of a rectangular parallelepiped-shaped aluminium plate. The vibration spectrum gives the lowest natural frequencies of the sample. Assumption that the vibration of the plates may be described by some approximate theories is proven to be inconsistent. The Ritz method, with products of powers of the co-ordinates as basis functions, is applied to obtain the lowest flexural natural frequencies. Three-dimensional solutions are obtained, unlike those provided by simpler theories. The experimental results are compared with the numerical predictions and a good agreement is obtained. Finally, forced motion is applied to the centre of the plate and the out-of-plane and in-plane displacement components for the first symmetric mode are measured. A good fit of the calculated values to the experimental values is found.

1. Introduction

Vibration of elastic plates has been widely studied, both from experimental and theoretical points of view [1–4], since plates are important components in many engineering applications. A vast literature exists for the flexural vibration of rectangular plates. Vibration of a plate can be

*Corresponding author. Tel.: +34-91-3367072; fax: +34-91-3366952.
E-mail address: abayon@dfarn.upm.es (A. Bayón).

0022-460X/$ - see front matter © 2003 Elsevier Ltd. All rights reserved.
doi:10.1016/j.jsv.2003.10.046

excited and detected with an appropriate experimental set-up. A correct interpretation of the results leads to useful information on elastic properties of materials and structural vibrations.

The classical theory of Kirchhoff assumes that plane sections remain plane and perpendicular to the mid-plane. Although many developments in approximate theories have occurred, the approach that has become prevalent was first applied to plates by Mindlin [5]. His theory includes the shear and rotary inertia effects.

The Ritz method is one of several possible procedures for obtaining approximate solutions for the frequencies and modes of vibration of elastic plates. It was applied by its inventor to the study of free vibration of a plate a century ago [6]. The Ritz method proposes a suitable set of basis functions, depending on the co-ordinates. The displacements are assumed to be a sum of such functions multiplied by constant coefficients. The Ritz method, with use of beam functions [7,8] and characteristic orthogonal polynomials [9], has been applied to obtain the flexural natural frequencies of thin rectangular plates giving good results. In order to study the free vibration of Mindlin plates, Dawe and Roufaeil [10] apply the Ritz method with Timoshenko beam functions as admissible functions for the displacements. The referred works do not deal with the general problem of displacements which depend on the three co-ordinates. The approximate solutions yield frequencies of sufficient accuracy for some engineering applications.

Three-dimensional (3-D) vibration analysis yields accurate results for thick plates. The solutions obtained show the range of applicability of the classic plate and Mindlin plate theories. Hutchinson and Zillmer [11] used a series solution of the general equations of linear elasticity to determine natural frequencies of vibration of a rectangular parallelepiped plate. In a paper by Liew et al. [12], the Ritz formulation is applied to the vibration analysis of thick rectangular plates; the displacements are expressed by sets of orthogonally generated polynomial functions. Lim [13] investigated the effects of neglecting transverse normal stress in the vibration analysis for a cantilevered parallelepiped plate. The results show that transverse normal stress becomes significant for large thickness ratios. 3-D solutions for cantilevered parallelepipeds have been derived by Leissa and Zhang [14]. Such solutions are obtained by the Ritz method with algebraic polynomials. Because of the relative simplicity of the algebraic polynomial displacement functions, the differentiations and integrations can be carried out exactly. The polynomial series chosen does not affect convergence directly [15].

Many articles have been published on experimental studies of vibration of plates. Most of the experimental papers are concerned with the characterization of vibration modes using accelerometers [16,17]. Therefore, detection is through contact and the average out-of-plane displacement component of the detection area is measured. Optical methods have also been applied in order to study the vibration. The out-of-plane displacement component of a vibrating cylinder has been accurately detected by a laser interferometer [18]. Low et al. [19] use a TV-holographic system as a detector of the vibration and Ritz's method with unidirectional displacements for non-free plates. The detection is qualitative: the mode shapes show the nodes and the amplitude distribution, but the total deformation is not quantified. The work by Ma and Lin [20] accounts for the detection of only the out-of-plane displacements of a vibrating plate by electronic speckle interferometry and excitation by a glued transducer; mode shapes are represented by lines of constant amplitude.

The present paper reports an almost free vibration of an aluminium plate generated by a percussion. The lowest natural frequencies are obtained from an accurate detection of the

out-of-plane displacements by laser interferometry. In contrast to the aforementioned studies, experimental research of the first mode shape and the lowest natural frequencies is carried out by detecting both the out-of-plane and in-plane components of the displacement components with a sensitivity of approximately 1 nm by means of an I/O laser interferometer, i.e. detection is two-dimensional, point-like and without contact.

The establishment of a method to estimate the error of the experimental measures permits the calculation of systematic uncertainties of the elastic constants and frequencies.

It is analytically demonstrated that the vibration of the plate cannot be described exactly in terms of displacements perpendicular to its plane nor in terms of Kirchhoff theory or Mindlin theory.

3-D vibration modal analysis is performed here by means of the Ritz method. In the application of this method, series of products of the co-ordinates to certain powers are used as basis functions. This selection is correct from the mathematical point of view as well as suitable from the conceptual point of view. The Ritz method is implemented in Maple on a PC. A straightforward procedure, a didactic series, and an easily adjustable program have been developed. Three approaches are studied using the Ritz procedure to find the simplest and best solution for the displacements: one where the Kirchhoff theory is assumed, another where the Mindlin theory is applied, and the third where displacement components dependent upon the three spatial co-ordinates, 3-D method. The error of the frequency numerical calculations due to the elastic constants and dimensional uncertainties is estimated.

Comparison of experimental and numerical results permits the validation of the accuracy of both methods. Taking the respective frequency uncertainties into account, the experimental results and the numerical predictions intersect for the two lowest natural frequencies, whereas a difference smaller than 0.5% is found for the third frequency.

When the plate is set into vibration by applying a periodic force to its centre, both the out-of-plane and the in-plane displacement components for the first symmetric mode are measured. The experimentally detected mode shape for the lowest frequency is in agreement with the theoretical predictions.

2. Experimental set-up and results

An aluminium plate, rectangular parallelepiped-shaped, with dimensions width $L_1 = 0.09990$ m, length $L_2 = 0.15100$ m, and thickness $L_3 = 0.02490$ m, is used for the tests in the laboratory. The mass m of the sample is 0.9951 kg, and its density $\rho = 2649\ \mathrm{kg/m^3}$. Fig. 1 shows a sketch of the plate and the set of co-ordinate axes OX_1, OX_2, and OX_3, with its origin O coincident with the centre of the plate. A point of the plate is determined by its co-ordinates x_1, x_2, x_3.

The P- and S-wave velocities are measured in the aluminium plate by the pulse-echo method in order to evaluate the elastic constants. The transit times for a path length of 2×0.02490 m is $t_p = 8.030 \times 10^{-6}$ s and $t_s = 15.588 \times 10^{-6}$ s for the P- and S-wave respectively. Consequently, the velocities are equal to $c_p = 6202$ m/s and $c_s = 3195$ m/s. From the expressions for c_p and c_s in terms of G and ν, $c_p = (G/\rho)^{1/2}[2(1-\nu)/(1-2\nu)]^{1/2}$, $c_s = (G/\rho)^{1/2}$, and from the definitions $c_p = 2L_3/t_p$ and $c_s = 2L_3/t_s$, the elastic constants can be determined from the relations:

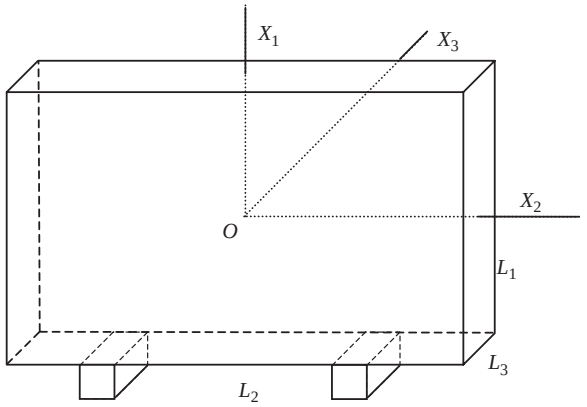

Fig. 1. The tested aluminium plate, with dimensions $L_1 = 99.90$, $L_2 = 151.00$, $L_3 = 24.90$ mm. An impact at the central point, $x_3 = -L_3/2$, induces vibrations, detected at $x_3 = L_3/2$. The plate is supported on two small rubber blocks.

- Shear modulus

$$G = \rho c_s^2 = \frac{4mL_3}{L_1 L_2 t_s^2}. \tag{1}$$

- The Poisson ratio

$$v = \frac{(c_p/c_s)^2 - 2}{2(c_p/c_s)^2 - 2} = \frac{(t_s/t_p)^2 - 2}{2(t_s/t_p)^2 - 2}. \tag{2}$$

The magnitudes measured directly in the laboratory appear explicitly in the right-hand terms of Eqs. (1) and (2). The values of the elastic constants obtained for the aluminium plate are $G = 27.04$ GPa and $v = 0.3194$ (Young's modulus being $E = 71.35$ GPa).

The experimental set-up for quasi-free vibration is shown in Fig. 2. The plate is placed with the face on the plane $x_3 = L_3/2$ in front of the detection system and it is supported on two small rubber blocks. Therefore, its movement is softly restrained. Symmetrical flexural vibration is induced by applying an impact perpendicular to the plate at the central point, $x_1 = x_2 = 0$, $x_3 = -L_3/2$. Symmetric modes mean that the third displacement component u_3 is symmetric with respect to the planes X_1OX_3 and X_2OX_3.

A pendulum consisting of a thread and a steel sphere is used to strike the sample. This type of excitation allows the plate to oscillate freely in its natural flexural modes, since following the impact, no further forces act upon the sample. In other words, once the impact has finished, the sample vibrates quasi freely, so that the vibration is not due to continuous action from external forces, as is common in conventional methods. The sphere is 3.45 mm in diameter. The time for the sound to go and to come back through the sphere may be estimated in 1 μs. Therefore the bandwidth is about 1 MHz, much more than the highest frequency found in the experiments described. To estimate better the bandwidth caused by the ball used to excite the vibration, a theory of impact of two solid spheres is applied [21]. To simplify, suppose that both the ball and

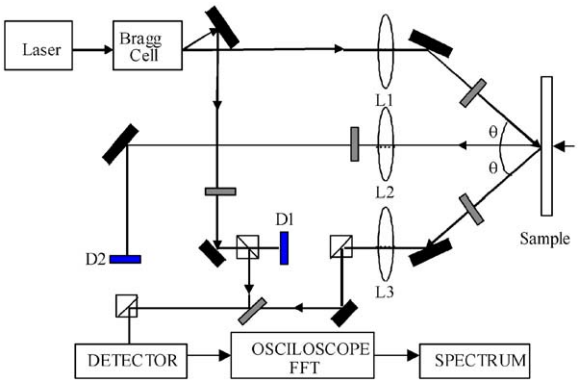

Fig. 2. The experimental set-up for detection of out-of-plane displacement. The unshifted laser beam is focused on the sample by the lens L1. The scattered light, collected by the lens L3, interferes with the reference beam. The mirrors are drawn in thick black and the shutters D1 and D2 in thin black.

the plate are made of steel, $E = 200$ GPa, $v = 0.3$, $\rho = 7900$ kg/m^3, and that the velocity of the ball before the impact is $v = 0.6$ m/s. The size and mass of the ball are much smaller than those of the plate. When neglecting the ball radius and mass m_b, the impact duration time is calculated as $t = 3.78(m_b^2(1-v^2)^2/(R_b E^2 v))^{1/5} = 13 \times 10^{-6}$ s. Hence the maximal excited frequency to be expected is 74 kHz. This bandwidth is adequate to excite the lowest natural frequencies of the plate.

A laser interferometer OP-35 I/O (Ultra Optec Inc.) [22] detects the resulting vibration at the central point, $x_3 = L_3/2$. This system permits the detection of both out-of-plane and in-plane displacement components at a point, though not simultaneously, with a resolution in amplitude of about 1 nm. Both components of the displacements are measured in this paper for flexural oscillations. The detection principle is based on the speckle phenomenon, which is observed when coherent light strikes on a scattering surface producing a pattern with bright and dark spots. The size of the illuminated area is approximately 20 μm; consequently, detection is point-like and without contact. The bandwidth ranges from 1 kHz to 35 MHz, allowing simultaneous detection of several natural vibration frequencies.

The interferometer works in the out-of-plane configuration as is shown in Fig. 2. The laser beam is split in two by a Bragg cell; one with the same frequency as the original, the other with a frequency shifted by 40 MHz. The unshifted beam is focused on the surface of the sample. The resulting scattered light is collected in the direction symmetrical to that of the incident beam and is directed to the beam mixer where it interferes with the reference beam. An out-of-plane displacement δw, in the OX_3-direction, causes a phase change equal to $4\pi \cos\theta \delta w/\lambda_l$, where λ_l is the wavelength of the laser. A 40-MHz frequency signal, modulated in phase by the displacements, is obtained in the detector. The signal is processed by a demodulating unit to yield an output proportional to the instantaneous displacement of the surface at the detection point. Finally, a Tektronic TDS430A oscilloscope digitizes the signal and gives the spectrum of the vibration, calculated by using the fast Fourier transform (FFT). The natural frequencies will be those associated with the maximum amplitudes in the spectrum. The spectrum of the out-of-plane component obtained for the sample is that of Fig. 3. The lowest flexural frequencies

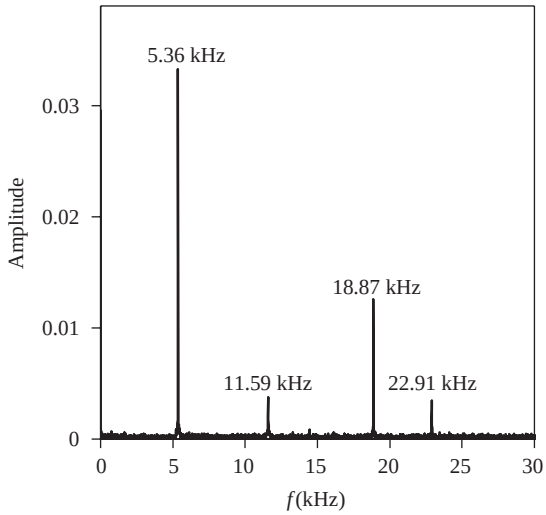

Fig. 3. The spectrum for the aluminium plate shows its first natural frequencies for flexural modes.

detected are $f_1 = 5.36$ kHz, $f_2 = 11.59$ kHz, and $f_3 = 18.87$ kHz. In the in-plane mode the unshifted and the shifted beams strike at the same point of the sample in symmetric directions. The scattered light is collected in the direction of the bisector corresponding to these directions, which coincides with the normal to the surface of the sample and later is processed. This operation mode will also be used in the detection of the mode shape.

The peaks of the spectrum shown in Fig. 3 may be fitted to a sinc function whose bandwidth provides the duration of the impact. A bandwidth of 3×10^4 Hz is estimated, which corresponds to a duration time of about 3×10^{-5} μs. This result confirms the goodness of the percussion apparatus. In order to check the freedom of the cylinder, four experiments are carried out corresponding to different locations of the supports. In a first series, the sample is supported on two small rubber blocks placed $0.17L_2$, $0.24L_2$, and $0.33L_2$ apart from both ends respectively. The detected frequencies are exactly the same for the three locations. When only a rubber block is located at the centre, the first and second frequencies have the same values as those detected with two rubber support. However, the third frequency sometimes differs from the value obtained in the first series by 0.2%.

3. Uncertainties

Since one of the objectives of this paper is to compare the experimental results with the theoretical ones, it would appear convenient to calculate the uncertainty of the experimental measures of directly or indirectly obtained magnitudes.

The systematic uncertainty methodology states that [23], if a physical magnitude y is a function, $y = F(\{x_i\})$, of a set of physical magnitudes x_i, which have been measured directly and they are affected by their respective uncertainties, U_{x_i}, then the uncertainty of an indirect measurement U_y is estimated by means of the differential of this function using the absolute values of the partial

derivatives, that is, $U_y = \Sigma|\partial F/\partial x_i|U_{x_i}$. It is supposed that all the measuring instruments are well calibrated and their uncertainties are only due to their sensitivities.

The uncertainties in the measurement of lengths, mass and transit times are 5×10^{-5} m, 10^{-4} kg and 10^{-9} s, respectively. From these, the absolute value of the systematic uncertainty in the indirect measurement of the shear modulus, deduced from Eq. (1), is $U_G = 0.08$ GPa. In the same way, from Eq. (2), the systematic uncertainty for the Poisson ratio is found to be $U_v = 0.0001$. These values obtained for the uncertainties of G and v must be considered minimum values, because neither random uncertainties nor calibration errors have been taken into account. Uncertainties U_G and U_v will be used in the determination of the systematic uncertainty for the frequencies calculated by Ritz's method.

The resolution of the used Fourier analyzer is 10 Hz. Hence the systematic uncertainty of experimental frequencies is 10 Hz for every value of the frequencies f_1, f_2, and f_3.

4. Non-3-D theories

As the general analytical calculation of the vibration normal modes and natural frequencies of a free plate is not possible, approximate solutions have been obtained historically.

The thickness L_3 of the plate is small with respect to the lengths of the other edges. Therefore some authors take as a fact, that the co-ordinate x_3 of the points of the plate do not require consideration [8,16]. Other authors [24] understand that it is only the displacement of the points of the plate belonging to the neutral surface in flexion which must be included in the calculations. In studying vibration of plates, it is sometimes an accepted assumption that the displacements are: $u_1 = u_2 = 0$, $u_3 = u_3\,(x_1, x_2, t)$. That is highly unreasonable because motion in the free plate would be too constrained.

The basic kinematics of the classical theory of thin plates is the same as that of Bernouilli–Euler beams [24]. If small deflection u_3 and slopes are assumed, the curvatures may be approximated by the partial derivatives of the deflection from the middle plane of the plate, $x_3 = 0$. In this case $u_3 = u_3(x_1, x_2, t)$, and the displacement components u_1 and u_2 may be written by the particular and simple expressions:

$$u_1 = -x_3\left(\frac{\partial u_3}{\partial x_1}\right)_{x_3=0}, \quad u_2 = -x_3\left(\frac{\partial u_3}{\partial x_2}\right)_{x_3=0}. \tag{3}$$

Mindlin assumed that u_1 and u_2 are proportional to x_3 and u_3 is independent of x_3:

$$\begin{aligned} u_1 &= x_3\varphi_1(x_1, x_2, t), \\ u_2 &= x_3\varphi_2(x_1, x_2, t), \\ u_3 &= \varphi_3(x_1, x_2, t). \end{aligned} \tag{4}$$

If the solution of motion of the plate is stated in this manner, an objection appears as demonstrated here.

The components of the fundamental equation of dynamics, Navier–Cauchy equation [24(1)], is

$$F_i + G\frac{\partial^2 u_i}{\partial x_j \partial x_j} + (G+\lambda)\frac{\partial}{\partial x_i}\left(\frac{\partial u_j}{\partial x_j}\right) = \rho\frac{\partial^2 u_i}{\partial t^2}, \tag{5}$$

where F_i are body forces, the displacements u_i are functions of class C^1, and λ is the second Lamé's elastic coefficient.

If body forces are null, $F_i = 0$, and a harmonic solution of Mindlin's type is assumed:

$$\begin{aligned} u_1 &= x_3 f_1(x_1, x_2)\sin(\omega t), \\ u_2 &= x_3 f_2(x_1, x_2)\sin(\omega t), \\ u_3 &= f_3(x_1, x_2)\sin(\omega t). \end{aligned} \tag{6}$$

The third component of Eq. (5) with Eqs. (6) gives

$$G\frac{\partial}{\partial x_1}\left(f_1 + \frac{\partial f_3}{\partial x_1}\right) + G\frac{\partial}{\partial x_2}\left(f_2 + \frac{\partial f_3}{\partial x_2}\right) + \lambda\left(\frac{\partial f_1}{\partial x_1} + \frac{\partial f_2}{\partial x_2}\right) = -\rho\omega^2 f_3. \tag{7}$$

At the boundary $x_3 = L_3/2$ the stress tensor is null and Hooke's law gives

$$0 = p_{13} = 2G\varepsilon_{13} = G\left(f_1 + \frac{\partial f_3}{\partial x_1}\right)\sin(\omega t), \tag{8}$$

where p_{ij} and ε_{ij} refer to the components of the stress and strain tensors respectively.

Therefore $f_1 + \partial f_3/\partial x_1 = 0$ at the boundary. As $f_1 + \partial f_3/\partial x_1$ is independent on x_3, it implies $f_1 + \partial f_3/\partial x_1 = 0$ for all the plate.

A similar argument for p_{23} gives $f_2 + \partial f_3/\partial x_2 = 0$ and $\partial f_1/\partial x_1 + \partial f_2/\partial x_2 = 0$ for p_{33}.

With these results, Eq. (7) implies that $f_3 = 0$, therefore $u_3 = 0$ for all the points of the plate. In other words, the plate does not move.

If solutions given by Eqs. (3) are assumed, a particular case of Eqs. (6) is

$$\begin{aligned} f_1(x_1, x_2) &\equiv -\frac{\partial f_3}{\partial x_1}, \\ f_2(x_1, x_2) &\equiv -\frac{\partial f_3}{\partial x_2}. \end{aligned} \tag{9}$$

Analogously, there is no motion in this case.

It is concluded that the last two hypotheses for the motion are not acceptable. In other words, the proposed motions are incompatible with dynamics equations and boundary conditions. The two displacements exposed as a hypothesis may at most be considered as a solution similar to that found in the strength of materials. Similar simplifications such as neglecting the transverse normal stress [13] are inherently erroneous. 3-D solutions for displacements of a vibrating plate should thus be sought, which is performed in the next section. 3-D analysis not only provides realistic results but also brings out physical insights, which cannot otherwise be predicted by any 2-D analysis [25].

When a plate vibrates with free boundary conditions, an expectable mode is the simplest one of symmetrical bending, where the points of the plate, belonging to the OX_2 axis before the deformation, present at an instant of the motion a shape similar to the curve s_1 drawn in Fig. 4. Since a plate is easily deformable in the shown shape, a very low frequency probably corresponds to this mode, becoming the first symmetric mode. Therefore, in a first approximation the wavelength is equal to the length L_2 of the plate. The expected normal modes s_1 (first symmetric), a_1 (first antisymmetric) and s_2 (second symmetric) from these elementary theories remind one of

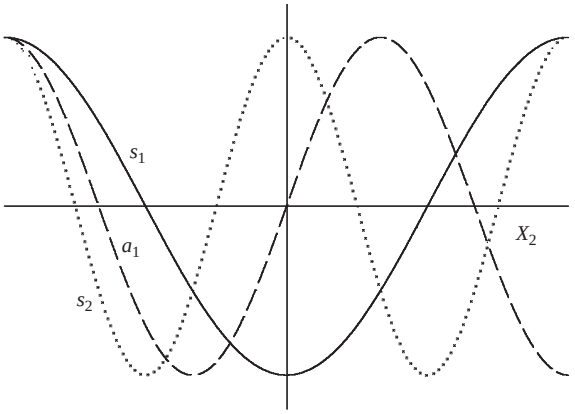

Fig. 4. Three vibration mode shapes given by the elementary theory for the lowest natural frequencies. The mode s_1 has the lowest frequency for the symmetric modes.

those drawn in Fig. 4. All the modes have maxima of amplitude on the edges and the symmetrical ones have another maximum at the centre. Since this paper is focused on the symmetrical modes, they are excited by applying an impact on the plate in a central point of one of its largest faces. In addition, as the displacements are also detected at the centre, the antisymmetrical vibration modes, possibly generated by lack of precision in the impact, are excluded. These reasons lead to impact and detection at the centres of opposite faces. Correct mode shapes are not known a priori, but it will always be true that symmetrical modes will have a maximum or antinode in the middle and antisymmetrical ones a null value or node at this point. Therefore the percussion and the detection must be done at the centres.

5. Ritz's method

Hamilton's principle postulates as the fundamental equation of dynamics for a free system that the integral between two given instants of Lagrange's functional of a system of particles is stationary. For a harmonic solution of the type $u_i = U_i\,(x_1, x_2, x_3)\sin(\omega t + \phi)$, $i = 1, 2$ and 3, it is enough to consider the maximum kinetic energy in a period of the motion

$$T_m = \tfrac{1}{2}\omega^2 \int_\tau \rho(U_1^2 + U_2^2 + U_3^2)\,\mathrm{d}\tau, \tag{10}$$

and the maximum potential energy

$$V_m = G \int_\tau \left(\varepsilon_{ij}\varepsilon_{ij} + \frac{v}{1-2v}\varepsilon_{ii}\varepsilon_{ii}\right)\mathrm{d}\tau, \tag{11}$$

where ρ, G, and v must be substituted by their aforementioned values, $\mathrm{d}\tau$ is a volume element, and ε_{ij} are calculated from U_i.

In Ritz's method, a solution for the displacements is proposed as a linear combination of a suitable set of basis functions [26] which satisfy the boundary conditions for the displacements, if

these are predetermined. Adequate functions, chosen here, are monomials formed by products of powers of the co-ordinates,

$$U_i = \sum_{pqr} A_{ipqr} x_1^p x_2^q x_3^r. \tag{12}$$

The formed algebraic polynomials have unknown coefficients $\{A_{ipqr}\}$, whose values are found by minimizing the difference between the maximum kinetic and potential energies, that is, the partial derivatives of such a difference with respect to each coefficient must be null,

$$\frac{\partial(T_m - V_m)}{\partial A_{ipqr}} = 0. \tag{13}$$

These conditions constitute a set of linear homogeneous algebraic equations in the unknown coefficients. The natural frequencies of vibration are obtained from the condition of compatibility of the set of equations, and the solution of the system gives the eigenvectors or coefficients. Substitution of Eqs. (12) into Eq. (10) yields its integrand as a function of x_1, x_2, x_3, and $\{A_{ipqr}\}$, hence a symbolic integration gives T_m as a function on $\{A_{ipqr}\}$ and ω^2. Substitution of Eqs. (12) into Eq. (11) yields V_m as a function on $\{A_{ipqr}\}$. The difference between the maximum kinetic and potential energies becomes a function on $\{A_{ipqr}\}$ and ω^2, hence the set of equations, Eq. (13), depends on ω^2 and $\{A_{ipqr}\}$. By introducing the nondimensional frequency parameter $\Omega = \frac{1}{2}\omega L_2\sqrt{\rho/G}$ the set of equations (13) may be written in matrix notation as

$$\mathbf{KA} = \Omega^2 \mathbf{MA}, \tag{14}$$

where $\mathbf{A}$ is the column matrix of the elements $\{A_{ipqr}\}$, $\mathbf{K}$ is the stiffness matrix and $\mathbf{M}$ is the mass matrix. The Maple program computes the eigenvalues and eigenvectors, i.e., the non-dimensional natural frequencies Ω and the corresponding coefficients $\{A_{ipqr}\}$ for each Ω.

The method has as an advantage that the solution can be obtained with the desired precision, except for the limitations of the computer and the spent time of computation. In addition, the obtained frequencies are always higher than the ones corresponding to the correct solution, reason why a more accurate value is found by simply adding a new term to the polynomial.

The expected most important displacement in flexural symmetric vibration of the plate is u_3. Therefore the exponents in the polynomial for U_3 must be high.

For flexural symmetric vibration modes the exponents of the co-ordinates in formula (12) for U_1 are successively odd, even, odd, while in the formula of U_2 are even, odd, odd and in the one of U_3 they are even, even, even.

A Maple program is developed to apply Ritz's method to the study of the free vibrations of a plate. The above-mentioned monomials are taken as the basis functions. For the validation of the program, the problem of vibrations of a cube, which has already been solved by the Ritz method with Legendre polynomials as well as verified experimentally [27] is solved. It is found that there is close agreement for the frequencies calculated for the lowest modes, which confirm the goodness of the program. The computer used is a PC, Pentium II.

In order to obtain the best and simplest solution for the flexural displacements of the vibrating plate, three different approaches to the problem are proposed:

(A) In a first approach, the amplitude U_3 given in Eqs. (15) is proposed and substituted into the approximate Eqs. (3). This yields the following displacements, corresponding to the classical thin

plate theory (Kirchhoff plate theory):

$$U_1 = -x_3 \sum_{p=0,q=0}^{P-1,Q} pA_{3pq} x_1^{p-1} x_2^q,$$

$$U_2 = -x_3 \sum_{p=0,q=0}^{P,Q-1} qA_{3pq} x_1^p x_2^{q-1},$$

$$U_3 = \sum_{p=0,q=0}^{P,Q} A_{3pq} x_1^p x_2^q. \tag{15}$$

With the maximum values for the exponents $P = 8$ and $Q = 8$, which means 25 unknown coefficients, the three smallest symmetric frequencies are 5851, 13 850, 24 408 Hz respectively.

(B) In a second approach, a linear in x_3, Mindlin assumption [28], Eq. (4), is studied:

$$U_1 = x_3 \sum_{p=1,q=0}^{P_1,Q_1} A_{1pq} x_1^p x_2^q,$$

$$U_2 = x_3 \sum_{p=0,q=1}^{P_2,Q_2} A_{2pq} x_1^p x_2^q,$$

$$U_3 = \sum_{p=0,q=0}^{P_3,Q_3} A_{3pq} x_1^p x_2^q. \tag{16}$$

With the maximum exponents: $P_1 = 3$, $Q_1 = 2$, $P_2 = 2$, $Q_2 = 3$, $P_3 = 6$, $Q_3 = 6$, after few seconds of computing time, the three lowest frequencies result: 5692, 12 971, and 22 965 Hz.

(C) In a third approach, the general case is studied. Displacements are assumed to be 3-D and to depend on the three spatial co-ordinates and time (3-D theory).

Considering the symmetries of the problem in the solution, a 3-D solution is given by:

$$U_1 = \sum_{p=1,q=0,r=1}^{P_1,Q_1,R_1} A_{1pqr} x_1^p x_2^q x_3^r,$$

$$U_2 = \sum_{p=0,q=1,r=1}^{P_2,Q_2,R_2} A_{2pqr} x_1^p x_2^q x_3^r,$$

$$U_3 = \sum_{p=0,q=0,r=0}^{P_3,Q_3,R_3} A_{3pqr} x_1^p x_2^q x_3^r. \tag{17}$$

With the smallest possible non-null values for P_1, $Q_1, \ldots, R_3$, that is $1,2,1;\ 2,1,1;\ 2,2,2$, respectively and after a computation time of half a minute, the obtained frequencies are 6018.6, 13 104.3 and 24 091.6 Hz. Repeating the calculation and after 5 h of computation, the three lowest frequencies 5345, 11 602, and 19 050 Hz were obtained, with the exponents up to 7, 6, 7; 6, 7, 7; 6, 6, 6, which means 192 unknown coefficients.

The systematic uncertainty in the numerical calculation of the frequencies in the 3-D solution is estimated by repeating the last calculation with the lengths of the sample increased, or decreased if it was required, by their corresponding uncertainties. The same process was repeated for the values of m, t_s and t_p. The absolute differences between the previously calculated frequencies and those obtained with shifted L, m and t have been considered as systematic uncertainties. These uncertainties originate from the lack of sensibility of measuring apparati and they have turned out to be 28, 62, and 91 Hz respectively for the three lowest natural frequencies.

Comparison of Eqs. (16) and (17) shows Eq. (16) as a particular case of Eq. (17) in which the maximum exponents R_1 and R_2 are unity and R_3 zero.

6. Symmetric mode frequency dependence upon thickness

In order to compare the quality of the different approaches studied, a calculation of natural frequencies of a plate as a function of its thickness is carried out. The approximations described by Eqs. (15)–(17) are applied to each thickness $L_3 = 24.9$, 20.0, 15.0, 10.0 and 5.0 mm. The numbers of unknown coefficients are 25 for Eqs. (15), 24 for Eqs. (16) and (17), that is, the computation times are of the same order. The results are given in Table 1.

The first row of Table 1 shows the five thicknesses studied. The first row of each sub-table shows the applied approach, given by the equations chosen and the maximum exponents of the co-ordinates x_1, x_2, x_3 taken: P_1, Q_1, R_1 for U_1; P_2, Q_2, R_2 for U_2; and P_3, Q_3, R_3 for U_3. The rest of the cells contain the first three lowest natural frequencies for each thickness and each approach. The sub-table corresponding to the approach A shows the three frequencies calculated by the

Table 1
The three lowest natural frequencies of a plate as a function of its thickness L_3

	L_3 (mm)				
	5.0	10.0	15.0	20.0	24.9
Approach A	Eqs. (15): 7, 8, 1; 8, 7, 1; 8, 8, 0				
f_1	1241	2464	3653	4792	5851
f_2	**3096**	6101	8935	11544	13850
f_3	**5879**	**11122**	**16139**	20607	24408
Approach B	Eqs. (16): 3, 2, 1; 2, 3, 1; 6, 6, 0				
f_1	1252	2469	3628	4712	5692
f_2	3124	**6067**	**8717**	**11027**	**12971**
f_3	6517	12083	16640	**20228**	**22965**
Approach C	Eqs. (17): 1, 2, 1; 2, 3, 1; 4, 4, 2				
f_1	**1182**	**2337**	**3441**	**4478**	**5420**
f_2	3308	6408	9168	11543	13519
f_3	6625	12336	16912	20481	23195

The approaches described by Eqs. (15), (16), and (17) are applied. The numbers of unknown coefficients are around 24. The first row of each sub-table shows the equations chosen and the maximum exponents of the co-ordinates x_1, x_2, x_3 taken. The lowest and best frequencies are typed boldface.

trial (15). The sub-table for the approach *B*, Eqs. (16), corresponds to Mindlin plates. The last sub-table (Approach C) corresponds to a simple 3-D theory. In all the three approaches it has been assumed that the displacement u_3 for low frequencies is predominant. Comparing the values of f_1 in Table 1 given by the approaches A, B, and C for thickness 5.0 mm, it is found that the value 1182 Hz results to be the lowest and therefore the best. This value, corresponding to the approach C, is typed boldface. Analogously the other lowest values of frequency for each thickness are marked in Table 1.

The tabulated values yield:

(1) Looking at the bold printed numbers in Table 1 it is deduced that for thin plates and high frequencies approach A, Eqs. (15), is the best. A reason for this conclusion may be that Eqs. (15) is based on the semi-analytic equations (3). Eqs. (3) becomes exact for plates with null thickness. Once more, a well-known statement is arrived at: Analytical solutions are the best.

(2) The first natural frequencies obtained with Eqs. (17) are lower than the frequencies calculated by Eqs. (15) and (16). Therefore, the solution obtained from Eqs. (17) seems better than that calculated from Mindlin theory for low frequencies.

(3) The results obtained with the few exponents chosen show that the best approximation depends on both the thickness and the frequency to be calculated. Fig. 5 shows the three lowest natural frequencies for each of the approaches A, B, C.

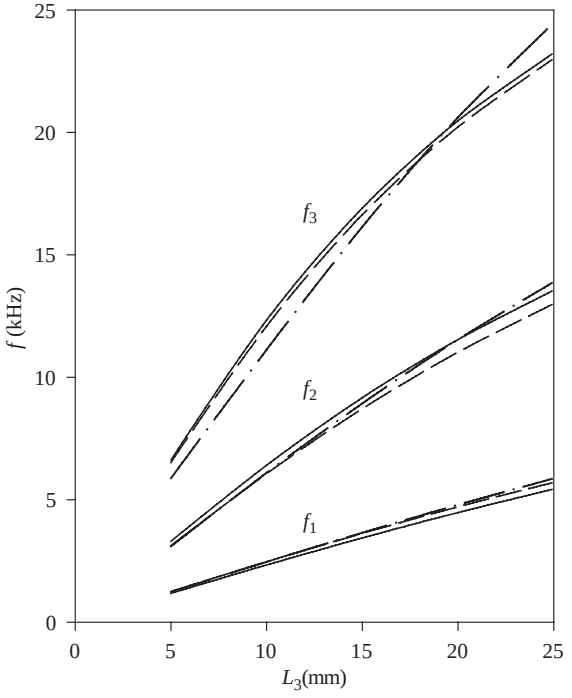

Fig. 5. Calculated natural frequencies (f_1, f_2, f_3) of a plate as a function of its thickness for a similar computation time: Dot-dashed lines for Kirchhoff theory (approach A), dashed lines for Mindlin theory (approach B), and solid lines for 3-D theory (approach C).

(4) At sight of (3), the first three natural frequencies for the aluminium test plate have been calculated with an increasing number of coefficients. For a number of coefficients given, the result depends on the election of the maximum exponents. With about 50 coefficients and estimating the optimal exponents, the three values are found to be smaller in the 3-D analysis than in Mindlin theory. Thus with optimal choice of exponents in 3-D theory (5,6,3;8,6,3;4,6,4), which corresponds to 100 coefficients, the calculated frequencies are 5345, 11 619 and 19 082 Hz. The frequencies are 5644, 12 791 and 20 043 Hz, when applying the theory of Mindlin, with an optimal election of exponents (9,12,1;10,11,1;8,10,0), that implies 101 coefficients. These results indicate differences higher than 5% in favour of the three-dimensional theory.

(5) Furthermore, if the number of coefficients increases, the 3-D theory will be the best, since an exact solution will be found.

7. Forced motion

A last experiment is carried out on the plate. The plate being supported as described before, a small transducer, 0.3 g in mass and 15 mm in diameter, is glued to the central point $x_1 = x_2 = 0$, $x_3 = -L_3/2$. A sinusoidal signal generator drives the transducer. By scanning the frequency around the lowest natural frequency (5360 Hz), the resonance frequency of the plate results 5346 Hz. The decrease in frequency below the natural frequency may be due to the added mass of the transducer. Twelve points, approximately 7 mm apart, on the straight line $x_1 = 0$, $x_3 = L_3/2$, and located at $x_2 = 0.08,\ 4.85, \ldots, 74.27$ mm are explored by the interferometer. Out-of-plane and in-plane motion of every point is detected, whereby both amplitude and phase are measured.

The measurement of the amplitude and phase of the displacement at a point of the lamina should be taken when the exciting frequency is near to the resonance. Therefore the displacement can be easily detected since a large amplitude is expected. However, if the exciting frequencies are too close to the resonance, any parasitic variation of frequency causes sharp changes of amplitude and phase. For this reason, a frequency of 5340 Hz is applied, which is similar to that of resonance but away from the peak.

Fig. 6 shows the out-of-plane and the in-plane displacements of three significant points. The three parts of Fig. 6 are obtained by averaging about a thousand scans. The maximum peak-to-peak displacement value is approximately 9 nm. Fig. 6(a) shows the out-of-plane displacement, u_3, and the in-plane displacement, u_2, of the point placed at $x_2 = 0.08$ mm from the centre. At this central point there is an antinode (maximum relative amplitude) for u_3 and a minimum for u_2. Fig. 6(b) shows the out-of-plane and in-plane displacements of the point placed at $x_2 = 39.2$ mm (from the centre). This point has a null amplitude U_3, which is a node for u_3. At the point placed at $x_2 = 74.27$ mm, very close to the edge of the plate, amplitude U_3 and amplitude U_2 reach a maximum, as is shown in Fig. 6(c). Fig. 7(a) shows the experimental amplitudes U_2 and U_3 (eigenvectors) pictured as arrows, for all 12 points.

In order to compare these experimental amplitudes, the Ritz method is applied with the approach C, which gives the lowest frequency $f = 5420$ Hz. The eigenvector corresponding to that first eigenvalue, substituted in Eqs. (17), gives the amplitudes U_2 and U_3 at $x_1 = 0$ and $x_3 = L_3/2$, for the 12 aforementioned points, with values of $x_2 = 0.08, 4.85, \ldots, 74.27$ mm. These

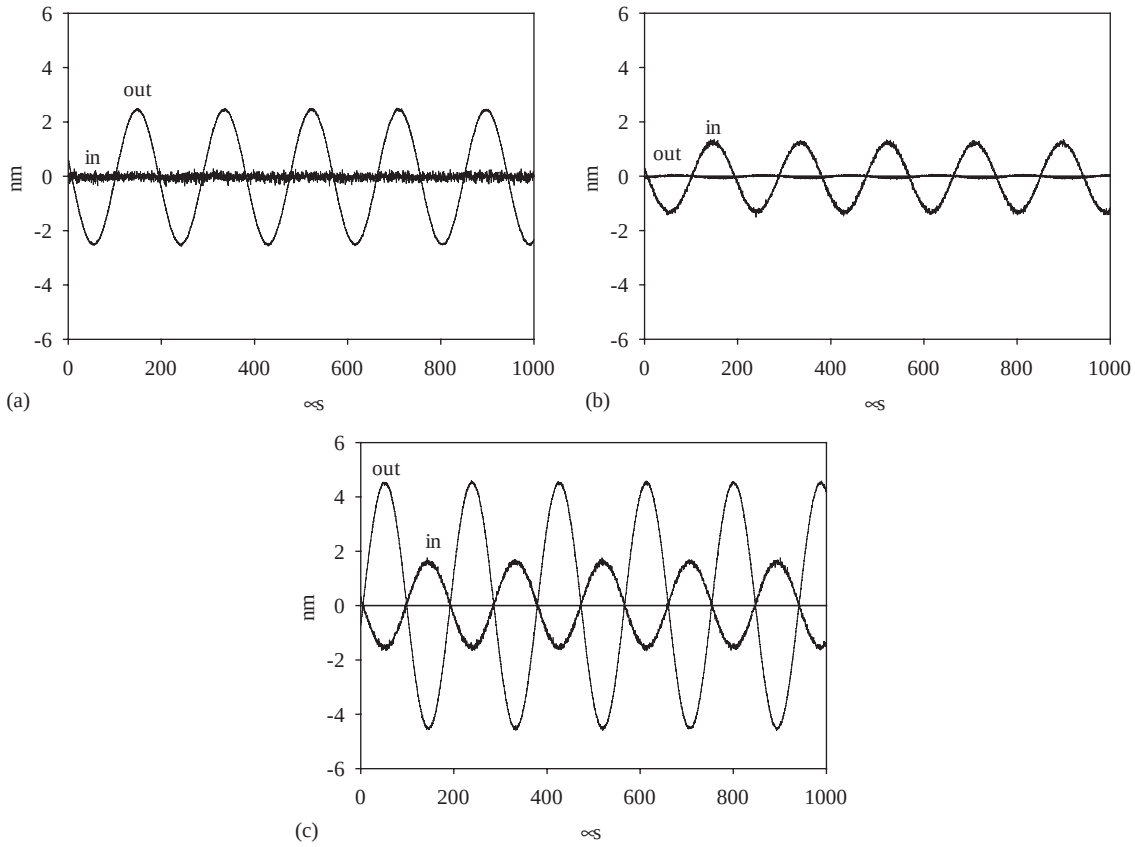

Fig. 6. The out-of-plane, u_3, and the in-plane, u_2, displacements of the three selected points at: (a) $x_2 = 0.08$ mm, (b) $x_2 = 39.2$ mm, and (c) $x_2 = 74.27$ mm. The maximum peak-to-peak displacement value is about 9 nm, corresponding to the out-of-plane amplitude at the edge.

amplitudes appear in Fig. 7(b), as 2-D arrows. Note the good agreement with respect to the experimental values shown in Fig. 7(a).

The vibration amplitude component U_3 is calculated by Eqs. (17) and approach C, for points in the surface $x_3 = L_3/2$. The results are drawn in Fig. 8 for the first lowest symmetric mode, $f = 5420$ Hz. An axonometric view is shown at the top; it reminds us of the symmetric mode s_1 supposed by elementary theory and drawn in Fig. 4. At the bottom of Fig. 8, a plot of isolines of U_3 on the surface $x_3 = L_3/2$ of the lamina is shown. A significant line is that of $U_3 = 0$, the nodal line, labelled with the symbol 0. This particular line allows qualitative comparison of its shape with that obtained experimentally by Waller [29], cited on [1(1)], on a brass plate; the shapes are very similar. Figs. 9 and 10 show the same kind of graphics for the second, $f = 13519$ Hz, and third, $f = 23195$ Hz, lowest symmetric modes, respectively. Fig. 9 is similar to the symmetric flexural mode of a beam parallel to the OX_1 axis and it is completely different in shape to the s_2 of Fig. 4. The shape of the third mode, Fig. 10, cannot be previewed by a rod theory.

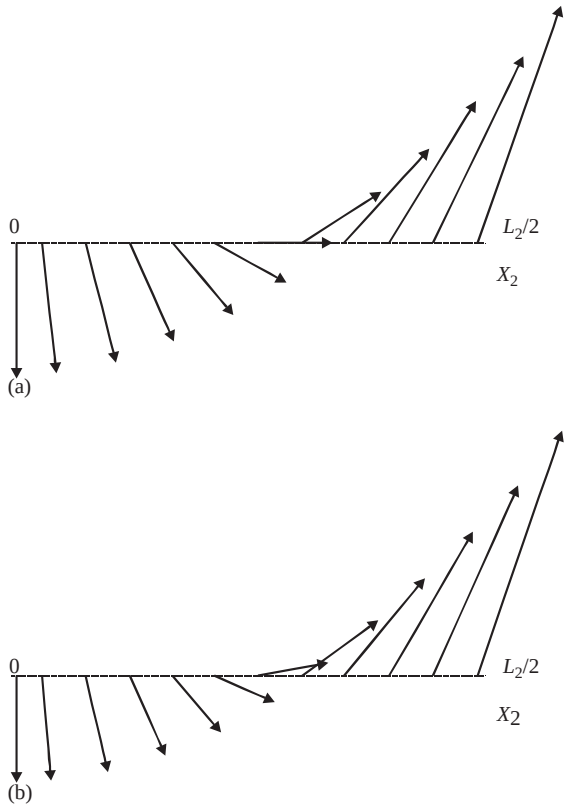

Fig. 7. (a) Experimental eigenvectors at the 12 analyzed points along the straight-line $x_1 = 0$, $x_3 = L_3/2$. Amplitudes and phases may be seen. (b) Numerical calculated values of the eigenvectors by Ritz's method. Note the agreement between the experimental and calculated values.

8. Conclusions

The main conclusions from the experimental and theoretical studies made on free flexural vibration of a lineal elastic plate and described in this paper, are

1. The assumption that in-plane displacements are proportional to the normal co-ordinate and the out-of-plane displacement is independent of the normal co-ordinate contradicts the laws of physics and therefore it is not admissible as an exact solution in any rectangular plate.
2. The application of Ritz's variational method to 3-D displacements yields the lowest vibration frequency of the tested plate, 5345 Hz, with a systematic uncertainty of 28 Hz, that is to say a relative systematic uncertainty of 0.5%. The second frequency is 11 602 Hz with its uncertainty 62 Hz and the third 19 050 Hz with 91 Hz.
3. The lowest quasi-free vibration frequencies of an aluminium plate are measured in the laboratory by speckle interferometry. The results are: 5.36, 11.59, and 18.87 kHz, with a sensitivity of 0.01 kHz.

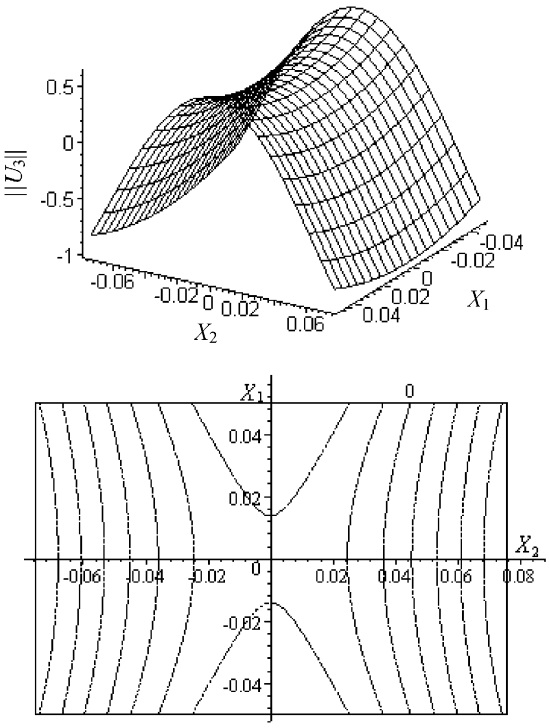

Fig. 8. Axonometric view and plot of isolines of U_3 on the surface $x_3 = L_3/2$ of the lamina, for the first lowest symmetric mode. Nodal lines, $U_3 = 0$, are labelled with the symbol 0 only on the first quadrant.

4. Taking into account all calculated uncertainties, the experimental results for the lowest frequencies are in good agreement with those obtained by numerical calculation. Note the coincidence of the experimental result 5.36 ± 0.01 kHz with the result of the 3-D theory, 5.345 ± 0.028 kHz. The second experimental frequency 11.59 ± 0.01 kHz also agrees with the calculated frequency 11.602 ± 0.062 kHz. The third experimental frequency 18.87 ± 0.01 kHz does not intersect the theoretical 19.05 ± 0.091 kHz by 0.5%, due to other uncertainty sources or non optimal choice of exponents in the Ritz method.
5. The in-plane and out-of-plane displacements experimental measurements give a symmetric mode shape for the lowest frequency in agreement with the theoretical prediction.
6. The coincidences expressed in conclusions 4 and 5 prove the accuracy of the experimental measurement by laser-interferometry to the same degree as do the numerical calculations by the Ritz method.
7. The general 3-D theory is equal to or better than the Mindlin theory for the same number of coefficients in the series, and hence for similar times of computation. Furthermore, if optimal exponents are chosen and the number of coefficients is great enough, the 3-D general theory will provide better results than Mindlin's one.

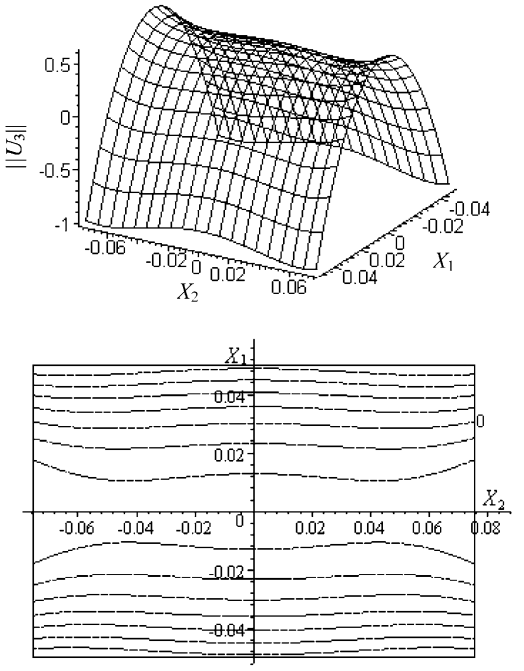

Fig. 9. Same as Fig. 8 for the second lowest symmetric mode.

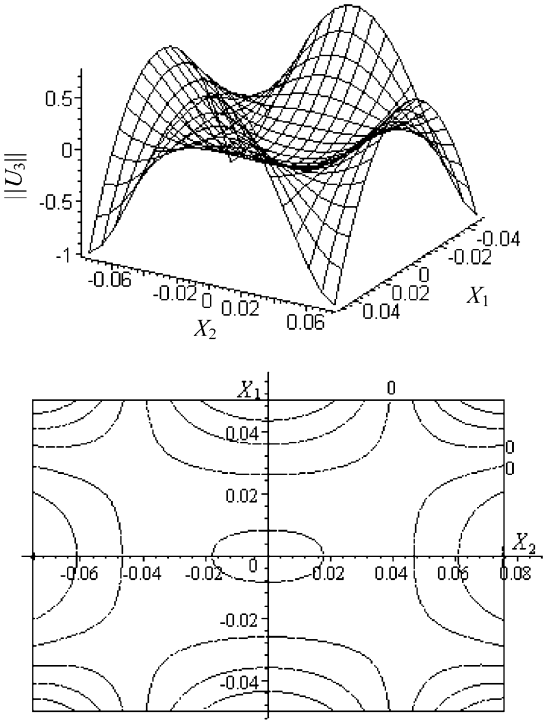

Fig. 10. Same as Fig. 8 for the third lowest symmetric mode.

References

[1] A.W. Leissa, *Vibration of Plates*, Acoustical Society of America, Woodbury, NY. 1993, Vol. 1, p. 115.
[2] W. Soedel, *Vibrations of Shells and Plates*, Marcel Dekker, New York, 1993.
[3] R. Szilard, *Theory and Analysis of Plates: Classical and Numerical Methods*, Prentice-Hall, Englewood Cliffs, NJ, 1974.
[4] D.J. Gorman, *Vibration Analysis of Plates by the Superposition Method*, Series on Stability Vibrations and Control of Systems, Vol. 3, World Scientific, Singapore, 1999.
[5] R.D. Mindlin, Influence of rotatory inertia and shear on flexural motions of isotropic, elastic plates, *Journal of Applied Mechanics* 18 (1951) 31–38.
[6] W. Ritz, Theorie der Transversalschwingungen einer quadratischen Platte mit freien Rändern (Theory of transversal motion of a square plate with free edges), *Annalen der Physik* 28 (1909) 737–786.
[7] A.W. Leissa, The free vibration of rectangular plates, *Journal of Sound and Vibration* 31 (1973) 257–295.
[8] D. Young, Vibration of rectangular plates by the Ritz method, *Journal of Applied Mechanics* 17 (1950) 448–453.
[9] R.B. Bhat, Natural frequencies of rectangular plates using characteristic orthogonal polynomials in Rayleigh–Ritz method, *Journal of Sound and Vibration* 102 (1983) 473–499.
[10] D.J. Dawe, O.L. Roufaeil, Rayleigh–Ritz vibration analysis of Mindlin plates, *Journal of Sound and Vibration* 69 (1980) 345–359.
[11] J.R. Hutchison, S.D. Zillmer, Vibration of a free rectangular parallelepiped, *Journal of Applied Mechanics* 50 (1983) 123–130.
[12] K.M. Liew, K.C. Hung, M.K. Lim, A continuum three-dimensional vibration analysis of thick rectangular plates, *International Journal of Solids and Structures* 30 (1993) 3357–3379.
[13] C.W. Lim, Three-dimensional vibration analysis of a cantilevered parallelepiped: exact and approximate solutions, *Journal of the Acoustical Society of America* 106 (1999) 3375–3383.
[14] A. Leissa, Z. Zhang, On the three-dimensional vibrations of the cantilevered rectangular parallelepiped, *Journal of the Acoustical Society of America* 73 (1983) 2013–2021.
[15] R.E. Brown, M.A. Stone, On the use of polynomial series with the Rayleigh–Ritz method, *Composite Structures* 39 (1997) 191–196.
[16] D. Larson, In-plane modal testing of a free isotropic rectangular plate, *Experimental Mechanics* 37 (1997) 339–343.
[17] R.K. Singal, D.J. Gorman, S.A. Forgues, A comprehensive analytical solution for free vibration of rectangular plates with classical edge conditions: experimental verification, *Experimental Mechanics* 32 (1992) 21–23.
[18] F.J. Nieves, F. Gascón, A. Bayón, Estimation of the elastic constants of a cylinder with a length equal to its diameter, *Journal of the Acoustical Society of America* 104 (1998) 176–180.
[19] K.H. Low, G.B. Chai, T.M. Lim, S.C. Sue, Comparison of experimental and theoretical frequencies for rectangular plates with various boundary conditions and added masses, *International Journal of Mechanical Sciences* 40 (1998) 1119–1131.
[20] C.C. Ma, C.C. Lin, Experimental investigation of vibrating laminated composite plates by optical interferometry method, *American Institute of Aeronautics and Astronautics Journal* 39 (2001) 491–497.
[21] L.D. Landau, E.M. Lishitz, *Theory of Elasticity*, Pergamon, Oxford, 1975, p. 36.
[22] J.P. Monchalin, J.D. Aussel, R. Heon, C.K. Jen, A. Boundreault, R. Bernier, Measurement of in-plane and out-of-plane ultrasonic displacements by optical heterodyne interferometry, *Journal of Nondestructive Evaluation* 8 (1989) 121–132.
[23] J.R. Taylor, *An Introduction to Error Analysis: The Study of Uncertainties in Physical Measurements*, University Science Books, Herndon, VA, 1982, pp. 70–74.
[24] K.F. Graff, *Wave Motion in Elastic Solids*, Dover Publications, New York, 1991, p. 229, (1) p. 274.
[25] D. Zhou, Y.K. Cheung, F.T.K. Au, S.H. Lo, Three-dimensional vibration analysis of thick rectangular plates using Chebyshev polynomial and Ritz method, *International Journal of Solids and Structures* 39 (2002) 6339–6353.
[26] S. Sokolnikoff, *Mathematical Theory of Elasticity*, McGraw-Hill, New York, 1956, p. 404.
[27] H.H. Demarest, Cube- resonance method to determine the elastic constants of solids, *Journal of the Acoustical Society of America* 49 (1971) 768–775.
[28] K.M. Liew, C.M. Wang, Y. Xiang, S. Kilipornchai, *Vibration of Mindlin Plates*, Elsevier, Amsterdam, 1998, pp. 5–6.
[29] M.D. Waller, Vibration of free rectangular plates, *Proceedings of the Physical Society, London* 72 (1949) 277–285.